



Fracture process zone and tensile behavior of blended binders containing limestone powder



Sumanta Das^a, Matthew Aguayo^a, Gaurav Sant^{b,c}, Barzin Mobasher^a, Narayanan Neithalath^{a,*}

^a School of Sustainable Engineering and the Built Environment, Arizona State University, Tempe, AZ, USA

^b Department of Civil and Environmental Engineering, University of California, Los Angeles, CA, USA

^c California Nanosystems Institute (CNSI), University of California, Los Angeles, CA, USA

ARTICLE INFO

Article history:

Received 16 December 2014

Accepted 3 March 2015

Available online 18 March 2015

Keywords:

CaCO₃ (D)

Pozzolan (D)

Fracture toughness (C)

Tensile properties (B)

Fracture process zone

ABSTRACT

Higher volumes of limestone can be used as OPC replacement by exploiting its increased reactivity in the presence of aluminous sources, thereby ensuring property-equivalence or improvements (e.g., strength, ionic transport). To examine the improvements in matrix fracture response in blended binder systems, this study characterizes and quantifies the flexural fracture process zone (FPZ) using digital image correlation. For the traditional OPC mortar, the localized strain intensity in the crack vicinity is the highest, FPZ initiates at a lower crack mouth opening displacement (CMOD), and its width is the lowest, while OPC–limestone–metakaolin blends show the lowest localized strain intensity, higher CMOD at FPZ initiation, and the highest FPZ width. The ultimate tensile strain and tensile toughness, extracted via inverse analysis, are found to be the highest for the ternary blends. The tensile modulus and the area under the softening region of the tensile constitutive relationship correlate well to the FPZ parameters.

© 2015 Elsevier Ltd. All rights reserved.

1. Introduction

Fine limestone is increasingly added to ordinary Portland cement (OPC) due to the sustainability benefits offered by a concomitant OPC reduction [1–4]. Incorporation of fine limestone facilitates better particle packing and provides nucleation sites for the hydration of OPC phases [5–7]. Limestone has also been observed to chemically combine with aluminum-provisioning materials such as fly ash or metakaolin to produce carboaluminate phases that improve the material microstructure and the properties [8,9]. This has resulted in methodologies that facilitate an increase in the limestone content in concretes beyond the ASTM compliance limit of 15%, especially in ternary binders which show beneficial changes in porosity and compressive/flexural strengths [3,10].

A recent study investigated the fracture properties of binary and ternary limestone blended matrices using notched beams in three-point bending and a two-parameter fracture model (TPFM) [10], and demonstrated that these matrices are more crack-tolerant. The crack-tolerance of such quasi-brittle materials is greatly influenced by the nature of stress transfer in the fracture process zone (FPZ). This complex nature of strain localization in the main crack as well as various secondary crack branches and micro-cracks is a major contributor to the non-linearity in quasi-brittle material fracture. The FPZ dissipates substantial energy through various mechanisms such as micro-cracking, crack-

deflection, crack bridging, crack-tip blunting, and crack-branching [11]. The resulting enhancement in toughness influences the durability of the material by enhancing its crack resistance. Hence this study addresses the crack propagation mechanisms in traditional OPC-based, and binary/ternary binder systems through monitoring the strain softening and strain localization behavior using the concept of FPZ. The dimensions of the FPZ and its evolution with load (and crack mouth opening displacement (CMOD), in a CMOD-controlled regime) are complex functions of the matrix microstructure and provide valuable information on matrix contributions to crack propagation and energy dissipation.

While several experimental techniques such as high speed photography [12], acoustic emission [13–15], scanning electron microscopy (SEM) [16–19], and laser-speckle interferometry [20,21] have been used to investigate FPZ in concretes, this study employs a non-contact digital image correlation (DIC)-based speckle-tracking method [10, 22–28] to assess the surface displacements and strains, and thus the width of the FPZ. The presence of soft(er) limestone particles and ductile clay phase (from metakaolin), which improves the fracture performance of multiple-material binders through improved inelastic energy dissipation [10], influences the FPZ, which is explored in detail. The tensile strengths and the ultimate tensile strains of these systems are extracted via inverse analysis of the flexural load-deflection data using an analytical tension model [29–32]. The tension-softening response of concrete is related to the FPZ characteristics [33]; thus a quantification of FPZ in such blended binder systems also provides unique indicators of their tensile properties.

* Corresponding author.

E-mail address: Narayanan.Neithalath@asu.edu (N. Neithalath).

Table 1
Chemical composition of the component materials.

Component (%)	Cement	Metakaolin	Fly ash
SiO ₂	21.0	51.7	58.4
Al ₂ O ₃	3.61	43.2	23.8
Fe ₂ O ₃	3.47	0.5	4.19
CaO	63.0	–	7.32
MgO	3.26	–	1.11
SO ₃	3.04	–	0.44
Na ₂ O	0.16	–	1.43
K ₂ O	0.36	–	1.02
LOI	2.13	0.16	0.50

2. Experimental program

2.1. Materials and mixture proportions

Commercially available type I/II ordinary Portland cement (OPC) conforming to ASTM C 150 is used in this study. The cement replacement materials include: Class F fly ash and metakaolin conforming to ASTM C 618, and limestone powders (CaCO₃ content greater than 97%) having median particle sizes (d_{50}) of 3 μm and 10 μm . The chemical compositions of OPC, metakaolin and fly ash are shown in Table 1. The particle size distributions (PSD) of 3 μm and 10 μm limestone powders are shown in Fig. 1(a) and those of OPC and the other replacement materials in Fig. 1(b). In order to obtain the amount of limestone particles for each median size required to match the PSD curve of the OPC, a least-squares fitting and error minimization procedure was implemented. The mass-based values obtained were 1.87% for 3 μm limestone and 98.13% for 10 μm limestone. This is not surprising because the PSD of the 10 μm median size limestone closely matches that of OPC as shown in Fig. 1(a).

Nine binary/ternary mortar mixtures were proportioned using OPC and the relevant replacement materials with a volumetric water-to-powder ratio, $(w/p)_v$, of 1.26 (the corresponding mass-based $w/p = 0.40$ for the control OPC mortar). The overall cement replacement levels used were 20% or 35% by volume. The mortars were prepared at a constant paste volume fraction of 50%. The silica sand used had an average particle size of 0.6 mm. The binder proportions and their nomenclature are shown in Table 2. The mortar mixtures were cast in prismatic molds (330 mm \times 76 mm \times 25 mm) for the determination of fracture properties. All the specimens were cured in moist conditions (RH > 98%) at a temperature of 23 ± 2 °C for 28 or 70 days before testing.

Table 2
The proportions of the binder materials used for the mortars.

Mix ID	Volumetric OPC replacement (%)	Contents of the binding materials (Vol. %)			
		Cement	Limestone	Fly ash	Metakaolin
OPC	0	100	0	0	0
LS 20	20	80	20	0	0
FA 20	20	80	0	20	0
LS 10 FA 10	20	80	10	10	0
LS 10 MK 10	20	80	10	0	10
LS 35	35	65	35	0	0
FA 35	35	65	0	35	0
LS 10 FA 25	35	65	10	25	0
LS25 MK 10	35	65	25	0	10

2.2. Determination of fracture characteristics

Three-point-bending tests were performed on notched beams as shown in Fig. 2. The depth of the notch was one-fourth of the beam depth, i.e., 19 mm. Four replicate beams (305 mm (span) \times 76 mm (depth) \times 25 mm (width)) were tested for each mixture. The test was performed using a closed-loop testing machine with the crack-mouth opening displacement (CMOD), measured using a clip gauge, acting as the feedback signal. The beams were monotonically loaded up to 111 N before shifting to CMOD-controlled mode. The CMOD-controlled mode was terminated at a CMOD value of 0.038 mm and the unloading stage was initiated by switching to load-controlled mode. The unloading was done with a constant unloading rate of 556 N/min up to a load of 89 N beyond which the CMOD-controlled mode was reintroduced. The second CMOD-controlled mode was continued till the CMOD value reached 0.16 mm. The mid-point deflections were also measured using a LVDT, as shown in Fig. 2.

DIC can be used to obtain full-field surface displacements through successive post-processing of digital images taken at specific intervals of time during the test. To provide contrast, the surfaces of the beams were speckled with random patterns. A charge-coupled device (CCD) camera was used to record images every 5 s (12 images per minute) as the specimens were being loaded/unloaded. The cameras were placed so as to image a rectangular area of approximately 120 mm \times 60 mm above the notch. After collection of all the images, the imaged area was analyzed. The correlation between the subsets of images from the deformed and undeformed state was determined in

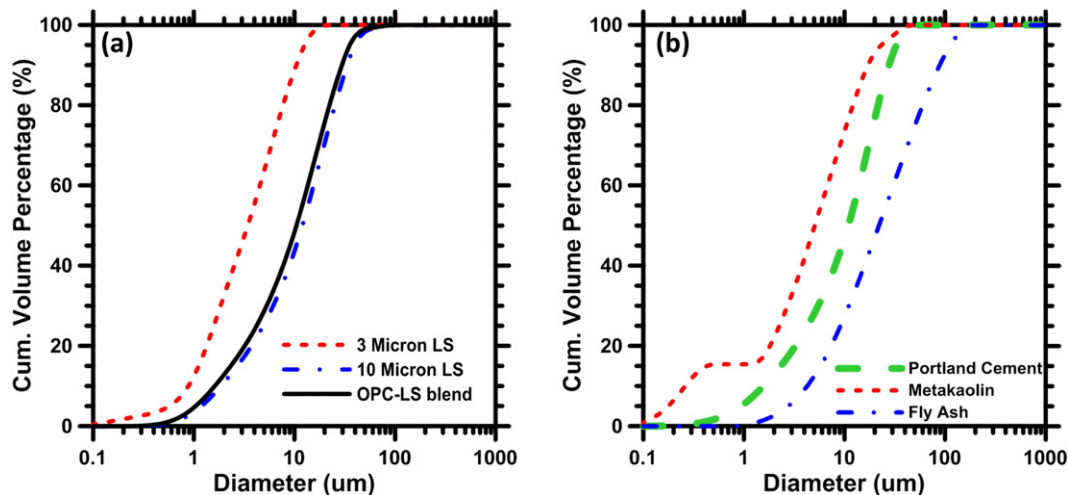


Fig. 1. Particle size distributions of: (a) limestone powders and, (b) cement, fly ash, and metakaolin, determined using dynamic light scattering technique.

Download English Version:

<https://daneshyari.com/en/article/1456134>

Download Persian Version:

<https://daneshyari.com/article/1456134>

[Daneshyari.com](https://daneshyari.com)